Available online at www.sciencedirect.com
ScienceDirect
Journal of the European Ceramic Society 26 (2006) 3477–3486
www.elsevier.com/locate/jeurceramsoc

Friction and wear behavior of C-based composites in situ reinforced with W_2B_5

Y. Lv [a], G. Wen [a,b,*], T.Q. Lei [a]

[a] School of Materials Science and Engineering, Harbin Institute of Technology, P.O. Box 433, Harbin 150001, China
[b] School of Materials Science and Engineering, Harbin Institute of Technology at Weihai, Weihai 264209, China

Received 9 June 2005; received in revised form 31 August 2005; accepted 10 September 2005
Available online 7 November 2005

Abstract

The C-W_2B_5 composites with W_2B_5 content of 30 vol.% and 40 vol.% were fabricated by reaction hot pressing sintering. The mechanical properties and friction and wear behavior of the composites were investigated. For comparison, the friction and wear behavior of graphite was also studied. It was found that the presence of W_2B_5 grain resulted in notable improvements in mechanical properties and wear resistance of the composites compared to graphite in spite of a little higher friction coefficient. A graphite-rich mechanically mixed layer (MML) was formed on the worn surface of the composites, which facilitated the low friction coefficient. Fracture and removal of the MML depending on the fracture toughness of the composites and Hertzian stress levels were considered to be the main wear mechanism.

Keywords: W_2B_5; Composites; Mechanical properties; Wear resistance

1. Introduction

Compared with other materials, carbon/graphite materials possess excellent high thermal stability, corrosion resistance, heat conduction and self-lubrication, and moreover retain their strength, modulus at elevated temperature.[1] So they have been widely applied in petrochemical engineering, machinery and aerospace fields as sealing elements.[2,3] Nevertheless, low strength and poor oxidation tolerance of the carbon/graphite materials could not meet the more and more severe challenge. For example, the sealing components used on the turbopumps and aero-engine that operate at higher speeds and pressures will experience higher pressure, flexural stress and temperature,[3,4] even than the ultimate values of carbon/graphite materials. Thus, improvement in the mechanical properties and resistance to wear and oxidation of the carbon/graphite materials are urgently required.

Despite the fact that an introduction of hard ceramics into carbon to form carbon/ceramics composites has improved the strength and oxidation resistance of carbon materials,[5–7] there are relatively few studies on the friction and wear behavior of such composites. However, it is reasonable to expect an increased wear resistance of this kind of materials because of the presence of hard ceramics and the increased strength and toughness, as compared with graphite. On the other hand, carbon/ceramics composites should have a lower friction coefficient due to the self-lubrication effect of carbon, as compared with ceramics, which is very important for many applications as moving components.

In our work, a new carbon/ceramics composite (C-W_2B_5) was proposed and prepared by reaction hot-pressing technique because of the excellent chemical and physical properties of W_2B_5, such as high melting point, high hardness, good corrosion resistance and anti-abrasion. In this article, the mechanical properties and friction and wear properties of this kind of materials were investigated.

2. Experimental

2.1. Materials preparation

The C-W_2B_5 composites were prepared from the starting powders of B_4C, WC and carbon black by hot-pressing at 2000 °C and 25 MPa for 1 h. The W_2B_5 and carbon were in situ

* Corresponding author. Tel.: +86 451 8641 8694; fax: +86 451 8641 3922.
E-mail address: g.wen@hit.edu.cn (G. Wen).

0955-2219/$ – see front matter © 2005 Elsevier Ltd. All rights reserved.
doi:10.1016/j.jeurceramsoc.2005.09.031

formed through the reaction between B_4C and WC powders, according to the following overall equation[8]:

$$5B_4C + 8WC = 4W_2B_5 + 13C \quad (1)$$

Based on this reaction formula, if the reaction is complete, the volume percentage of carbon in the C-W_2B_5 composites is about 30% that is not sufficient for many applications. The carbon black was added into the starting materials to produce high carbon content composites. In present work, the amounts of the W_2B_5 phase in the resulting materials were 30 vol.% and 40 vol.% respectively, and hereafter C-$x$$W_2B_5$ is used to refer to the C-W_2B_5 composite containing x vol.% W_2B_5. The starting compositions are listed in Table 1.

2.2. Characterisation

Bulk densities of the resulting materials were measured by using Archimedes' principle. X-ray diffraction and SEM were used to identify the reaction products and crack propagation path induced by the Vickers indenter, respectively. For mechanical testing, standard flexural bars with dimensions of 36 mm × 4 mm × 3 mm were cut from the hot-pressed bodies followed by a coarse and fine grinding, then the tensile faces were polished and the edges were beveled. Flexural strength was measured on a 3-point bending fixture with a 30 mm span at a crosshead speed of 0.5 mm/min. Samples used to measure fracture toughness with dimensions of 36 mm × 2 mm × 4 mm were notched a depth of 2 mm using a 100 μm thick diamond wheel. The K_{IC} values were determined by the SENB method with a crosshead speed of 0.05 mm/min. Each mechanical property data point represents an average of 5–6 measured values. The Vickers hardness tests were carried out under a load of 40 N.

2.3. Wear test

Dry sliding wear tests were conducted using a block-on-ring type machine. The samples were machined into rectangular blocks of 4 mm × 6 mm × 20 mm, and the faces of 6 mm × 20 mm were put in contact with the slider rings. The slider ring (out diameter 40 mm) was made of AISI 52100 type bearing steel with a bulk hardness of HRC63 ± 1. Prior to wear testing, all the contact surfaces were polished, cleaned in acetone in an ultrasonic cleaner and finally dried by blowing warm air. All the tests were carried out at room temperature with a relative humidity of ~30%. The normal loads F_N of 15 N, 35 N, 55 N and 75 N, and a constant line speed of 0.4 m/s were used. The sliding time for each test was normally 40 min. Wear tests were also performed on graphite at the same condition for reference. The friction torsion M was recorded every 30 s during each test, and the friction coefficient was calculated by the formula $\mu = M/R/F_N$, where R is the radius of the sliding ring. The width of the wear track were measured, and then the volume losses were calculated according to the formula (2)

$$V = \left(\frac{\arcsin(b/2R)}{180} \pi R^2 - \frac{b\sqrt{R^2 - b^2/4}}{2} \right) w \quad (2)$$

where V is the volume loss, b is the width of the wear track and w denotes the width of the specimen. The temperature of the contact surface was measured by a nickel chromium–nickel silicon thermocouple probe, inserted in the specimen through a hole near to the contact surface. After the wear test, the worn surfaces and wear debris were examined using a scanning electron microscope (SEM) coupled with EDX.

3. Results and discussions

3.1. Results

The reaction products of the sintered samples were first subject to XRD analysis. The results are shown in Fig. 1. Only the diffraction peaks of W_2B_5 and carbon were detected in the two specimens, no other compounds related with this system, such as B_4C, WC, WB and W_2B being present, confirming that the reaction between B_4C and WC was complete according to the reaction (1). The diffraction intensity of carbon was much weaker than that of W_2B_5 in each sample, which might be attributed to its low crystallization degree (compared with the diffraction peak of neat graphite (Fig. 1(a)). The bulk densities of the C-30W_2B_5 and C-40W_2B_5 specimens were about 4.9 g/cm^3 and 5.8 g/cm^3, respectively, and the relative densities were as high as 94.7% and 96.1%, as listed in Table 1.The high relative densities were considered to mainly come from the reaction sintering. The reaction produced newly formed W_2B_5 and carbon that had high sintering activities. In addition the reaction is exothermic ($\Delta H^0_{298} = -91930$ J, thermodynamic data are from the literature[9,10]), resulting in a relatively high actual sintering temperature. Both of these two effects promoted the densification of the materials. The results of mechanical properties of as-sintered materials are listed in Table 1. It is evident that the addition of W_2B_5 notably improved the mechanical properties of the composites compared with neat graphite. The flexural strength and fracture toughness of the C-40W_2B_5 composite were about five and seven times that of graphite, respectively. Moreover, the mechanical proper-

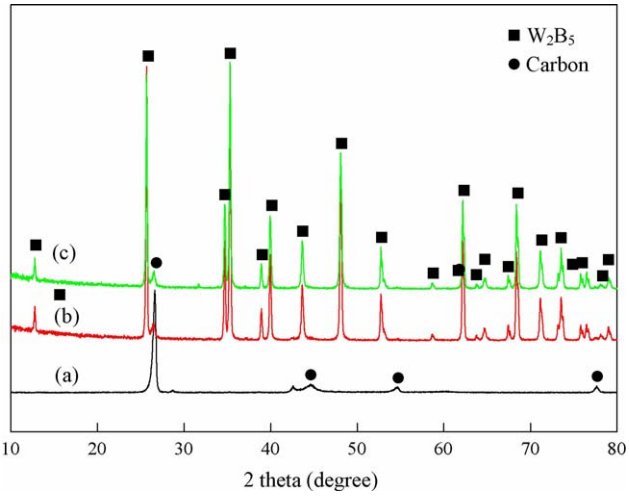

Fig. 1. XRD patterns of the C-W_2B_5 composites: (a) graphite; (b) C-30 W_2B_5; (c) C-40 W_2B_5.

Table 1
Starting compositions and properties of the C-W_2B_5composites and graphite

Materials	Starting compositions (vol.%)			Relative density (%)	Bulk density (g/cm^3)	Flexure strength (MPa)	Fracture toughness ($MPa\,m^{1/2}$)	Vickers hardness (GPa)
	B_4C	WC	Carbon black					
Graphite	–	–	–	–	–	52.5 ± 1.8	0.74 ± 0.1	–
C-30W_2B_5	19	17.5	63.5	94.7	4.9	165.9 ± 10.8	3.28 ± 0.1	1.08 ± 0.1
C-40W_2B_5	27.6	25.2	47.2	96.1	5.8	240.8 ± 25.6	5.07 ± 0.5	2.36 ± 0.1

ties of the composites increased with increasing W_2B_5 content. The high relative density, hard W_2B_5 grains and residual stress resulting from the difference of the thermal expansion coefficient between W_2B_5 and carbon are believed to contribute to the strengthening and toughening of the composites. In the C-40W_2B_5 composite, the W_2B_5 with grain size of about 1–2 μm fractured by a combination of intergranular and transgranular mode, as indicated at the points A and B in Fig. 2, which resulted in increased strength and toughness of the composite due to the high strength of W_2B_5 grains and crack deflection, as shown in Fig. 2. Furthermore, an isostatic tensile radial stress to the W_2B_5 grains and a compressive hoop stress and a tensile radial stress to the carbon matrix were generated because the thermal expansion coefficient of W_2B_5($7.8 \times 10^{-6}\,K^{-1}$)[11] is much greater than that of graphite ($\approx 2.5 \times 10^{-6}\,K^{-1}$).[12] As shown in Fig. 3, when the crack front encountered the W_2B_5 grain, under the synergetic action of the compressive hoop stress and tensile radial stress, the crack deflected from the original orientation and propagated along the direction parallel with compressive hoop stress and perpendicular to tensile radial stress. As the crack was close to the W_2B_5 grain, it directly deviated towards the W_2B_5 grain due to the increasing tensile radial stress in the matrix (the maximum value being at the interface of the carbon and W_2B_5), and reached the boundary of the W_2B_5 grain and the matrix, finally the crack propagated along the original orientation. The spreading path of the crack in the matrix lengthened, therefore leading to toughening.[13] And withal, the carbon grains with an average size of 0.16 μm estimated from the Eq. (3)[14] was much smaller than W_2B_5 grains, which resulted in a rather good toughening

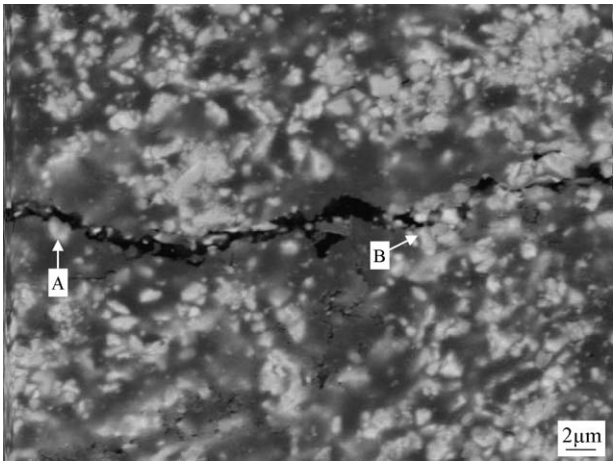

Fig. 2. SEM photograph of the crack propagation path of the C-40W_2B_5 composite induced by a Vickers indenter.

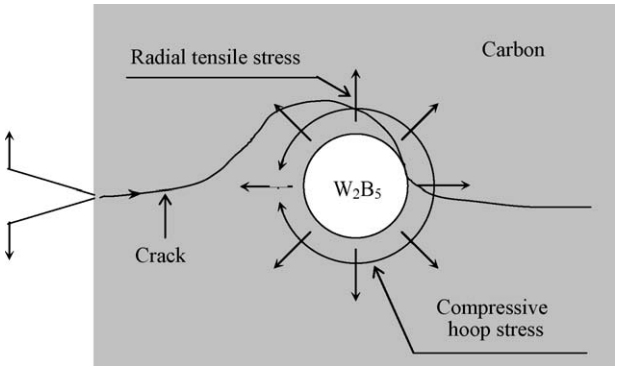

Fig. 3. Schematic diagram for the stress states in the composite and crack propagation path under residual stresses.

effect due to the longer crack deflection.[15]

$$L_a = \frac{9.5}{(d_{002} - 3.354)} \quad (3)$$

The representative friction traces of the C-W_2B_5 composites and graphite tested at low load of 15 N and high load of 75 N are shown in Fig. 4. The friction coefficients of all samples became somewhat constant after an initial increased period for any normal loads. The mean friction coefficients of the C-W_2B_5 composites and graphite at various loads are summarized in Table 2. It is clear that normal load and W_2B_5 content in the composites had great effects on the friction coefficient. As the load and W_2B_5 content increased, the friction coefficients of the samples were gradually increased. While for the C-30W_2B_5 composite, the friction coefficient was comparable to that of graphite, which suggested that within this volume percentage, the addition of W_2B_5 had little influence on the friction coefficient of the carbon-based composites.

Fig. 5 shows the wear rates of the graphite and C-W_2B_5 composites as a function of applied loads. It is clearly noted that the wear rates of the composites were much lower than that of graphite, as expected, especially at low loads (15 N and 35 N). For example, the wear rate decreased from $0.398 \times 10^{-3}\,mm^3/m$

Table 2
Friction coefficients of the graphite and C-W_2B_5 composites at different loads

W_2B_5 content (vol.%)	Normal load (N)			
	15	35	55	75
0 (Graphite)	0.139	0.194	0.205	0.214
30	0.185	0.201	0.223	0.234
40	0.241	0.274	0.341	0.389

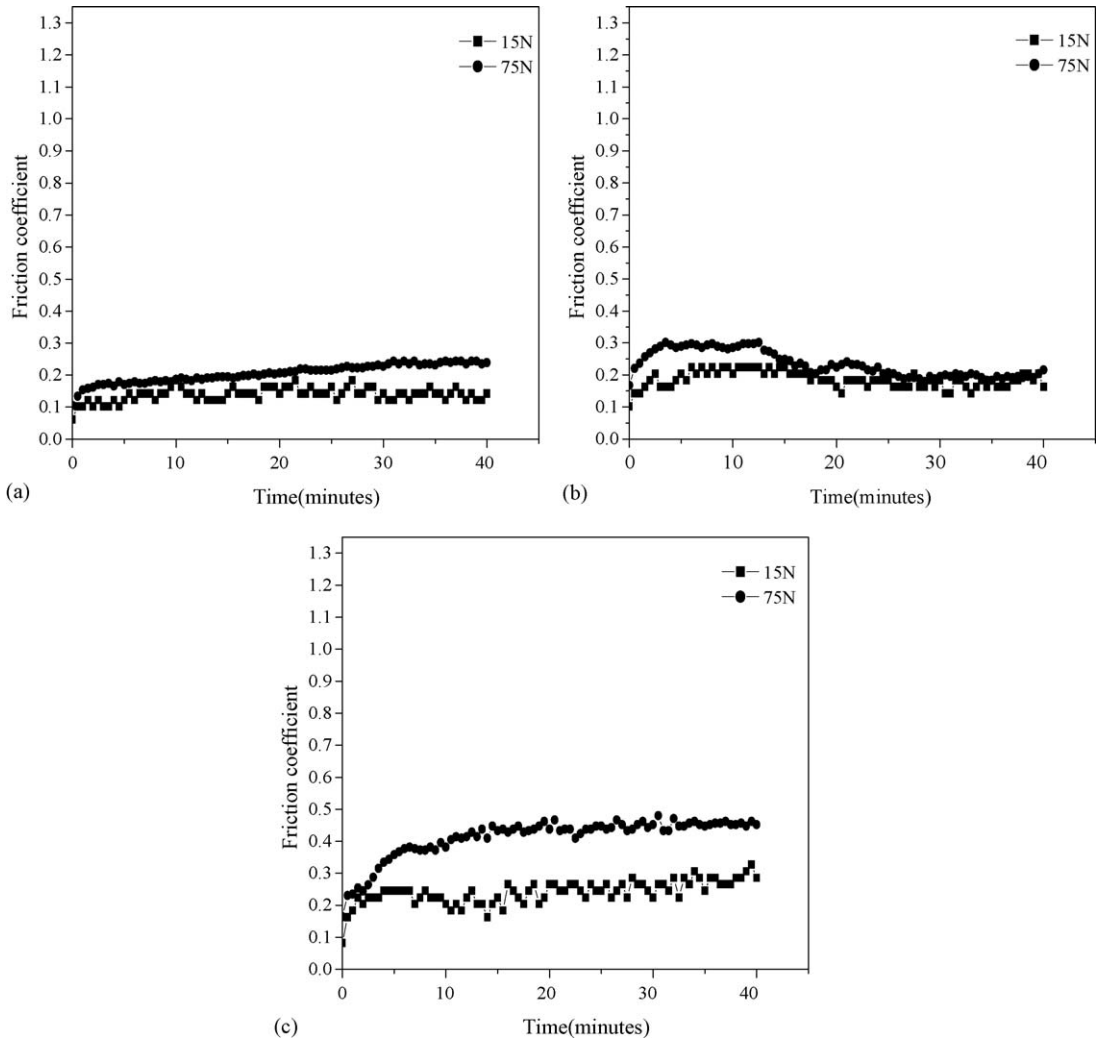

Fig. 4. Typical friction traces of the C-W_2B_5 composites and graphite: (a) graphite; (b) C-30W_2B_5; (c) C-40W_2B_5.

of the graphite to 0.066×10^{-3} mm^3/m of the C-30W_2B_5 composite when tested at 15 N. In addition, the wear rates increased with increasing applied load for all the materials. The wear rate of the C-40W_2B_5 composite was a little higher than that of the C-30W_2B_5 composite.

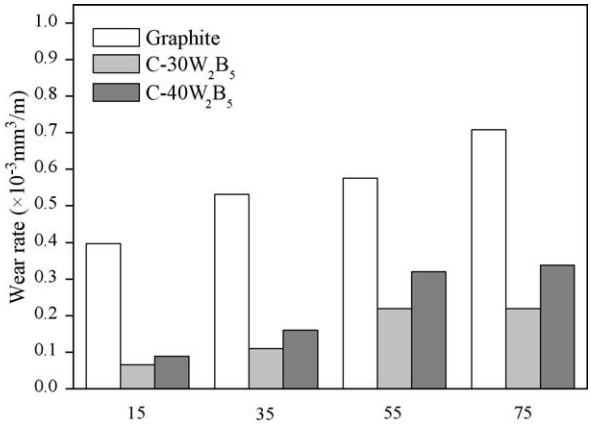

Fig. 5. Wear rates of the graphite and C-W_2B_5 composites at different loads.

The typical SEM photographs of the worn surfaces for the graphite and C-W_2B_5 composites at load of 15 N are shown in Fig. 6. In Fig. 6(a), a smooth film, coupled with some narrow and shallow furrows and blisters and cracks, was formed on the worn surface of graphite, which agrees with the works by Clark and Lancaster[16] and Blaw and Martin[17] The presence of furrows indicated the micro cutting of the counterface because the bearing steel is much harder than graphite. The blisters broke away as relatively large flakes of debris after the cracks connected and then left the surface damaged.[16] For the C-30W_2B_5 composite, the worn surface was covered with a continuous and smooth layer accompanying some white particles, irregular pits and small tilted flakes being breaking-off, as shown in Fig. 6(b). The EDX analysis (Fig. 7(a)) revealed that this smooth layer included elements of C, W, Fe and O, and the C content (81.32 at.%) was highest. The boron was not detected owing to the sensitivity limitation of the EDX to the light element B, but it was believed to be in the form of either W_2B_5 or B_2O_3 on the worn surface. Since this layer consisted of elements from C-W_2B_5 composites and bearing steel, as well as environmental matter, i.e. oxygen, it was defined as a "mechanically mixed layer" (MML).[18] Therein

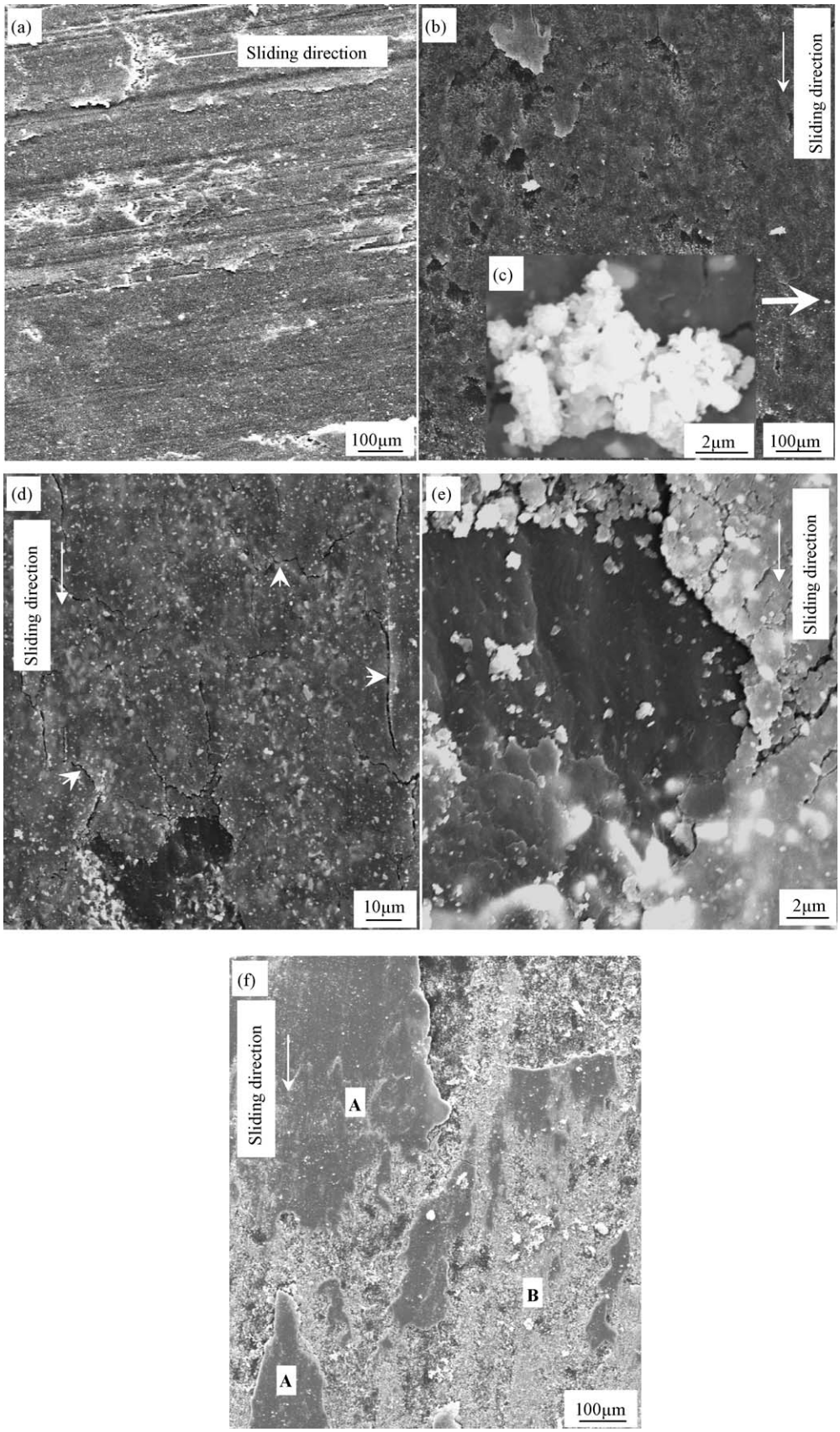

Fig. 6. SEM photographs showing the worn surfaces of the graphite and C-W_2B_5 composites: (a) graphite; (b) C-30W_2B_5 composite; (c) high magnified photograph of the white particle;(d) and (e) highly magnified photographs of the smooth layer and pit, respectively, in (b); (d) C-40W_2B_5 composite.

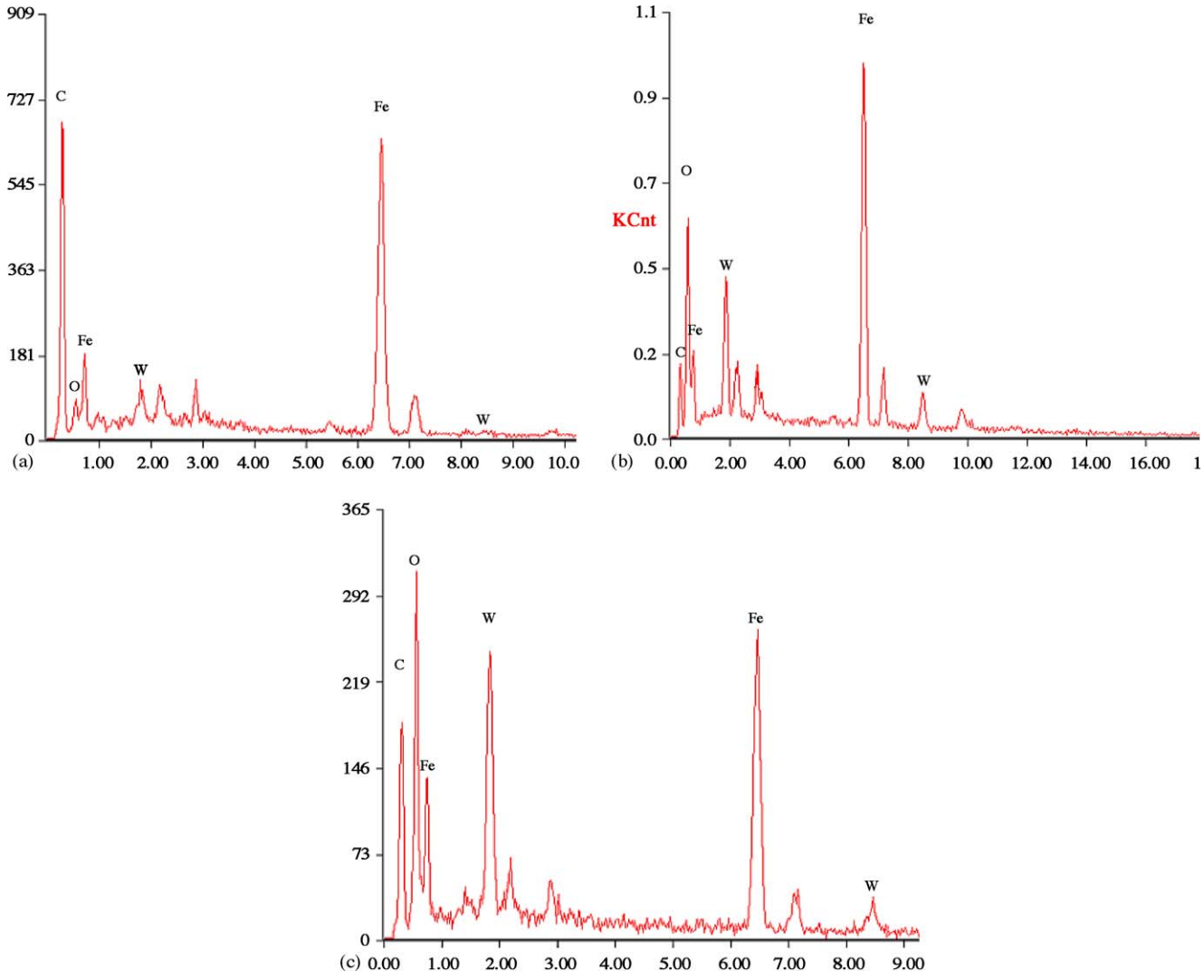

Fig. 7. EDX spectrums of the worn surfaces of the C-W_2B_5 composites: (a) C-30W_2B_5 composite; (b) white particle in Fig. 6(c); (c) C-40W_2B_5 composite.

to, Fe came from the counterpart, W and C from the composites, and O originated from the oxidation of the layer due to the friction heating. The high percentage of C indicated that this MML was a graphite-rich film providing the composite a lower friction coefficient and an excellent wear resistance. Such graphite containing lubrication film was also observed on the worn surfaces of ceramic-graphite and metal-graphite composites.[18–20] The white particles were an aggregation of fine debris with a grain size from 0.1 μm to 1 μm (Fig. 6(c)). The white particles also contained elements of W, Fe, C and O (Fig. 7(b)). As Observed in Fig. 6(d), the smooth MML presented many microcracks paralleling and interlacing the sliding direction (as pointed by short white arrows), which resulted from the surface fatigue similar to carbon-graphite materials,[16,17] while the pits were the fresh surfaces left by the removal of the tilted flakes as shown in Fig. 6(e).

The morphology of the worn surface for the C-40W_2B_5 composite was different from that of the C-30W_2B_5 composite. As shown in Fig. 6(f), besides the discontinuous and smooth graphite-rich MML (area A), the relatively rough film containing fine particles was on the worn surface (area B). From Fig. 7(c), it can be seen that the C content (59.05 at.%) on the worn surface of the C-40W_2B_5 composite decreased compared with C-30W_2B_5 composite, whereas Fe, W and O content increased, which indicated area B was rich in Fe, Fe_2O_3, W_2B_5 or oxide of tungsten and boron. The increase of the fine particles was attributed to the increase of hard W_2B_5 grains in the composite, which promoted the abrasive action between W_2B_5 and the counterpart. Simultaneously the friction coefficient of the tribo-system increased.[18,19] The comparison made on the surfaces of the bearing steel worn with the C-30W_2B_5 composite and C-40W_2B_5 composite, respectively, confirmed that more intensive rubbing took place in the tribo-system of C-40W_2B_5 composite (Fig. 8).

To investigate the influence of normal load on the wear behavior of the composites, SEM micrographs of the worn surfaces of C-30W_2B_5 composite tested at three applied loads were taken (Fig. 9). As discussed above, a continuous graphite-rich MML with small tilted flakes and microcracks was found on the worn surface of the C-30W_2B_5 composite when tested at 15 N (Fig. 6(b)), which noted that the graphite-rich MML was stable

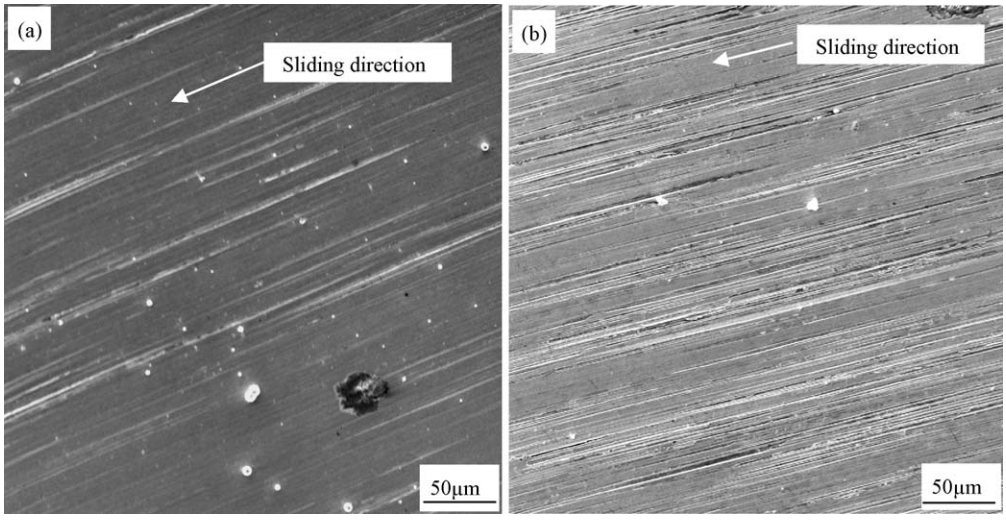

Fig. 8. SEM micrographs of the worn surfaces of the bearing steel at load of 15 N (a) against C-30W_2B_5 composite (b) against C-40W_2B_5 composite.

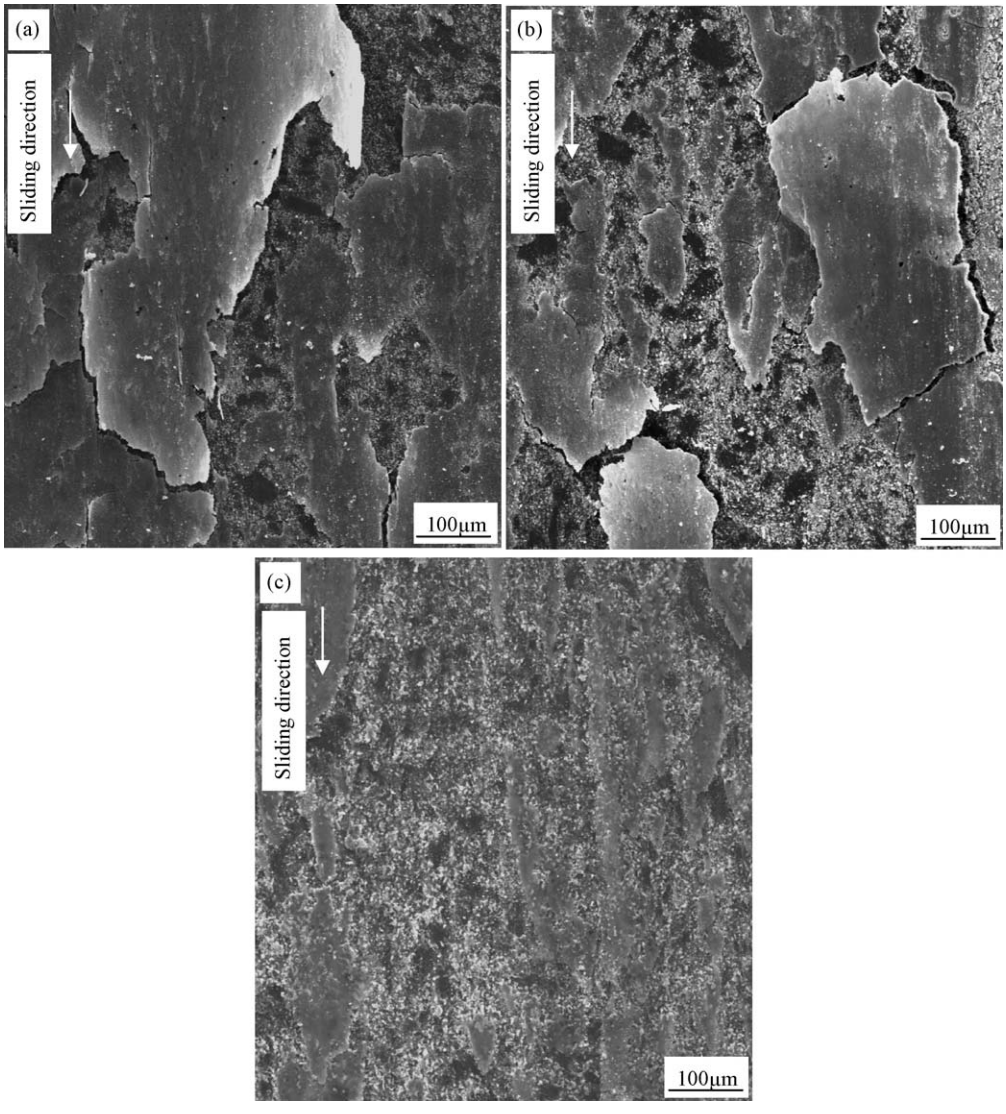

Fig. 9. SEM photographs of the worn surfaces of C-30W_2B_5 composites, wear tested at different loads: (a) 35 N; (b) 55 N; (c) 75 N.

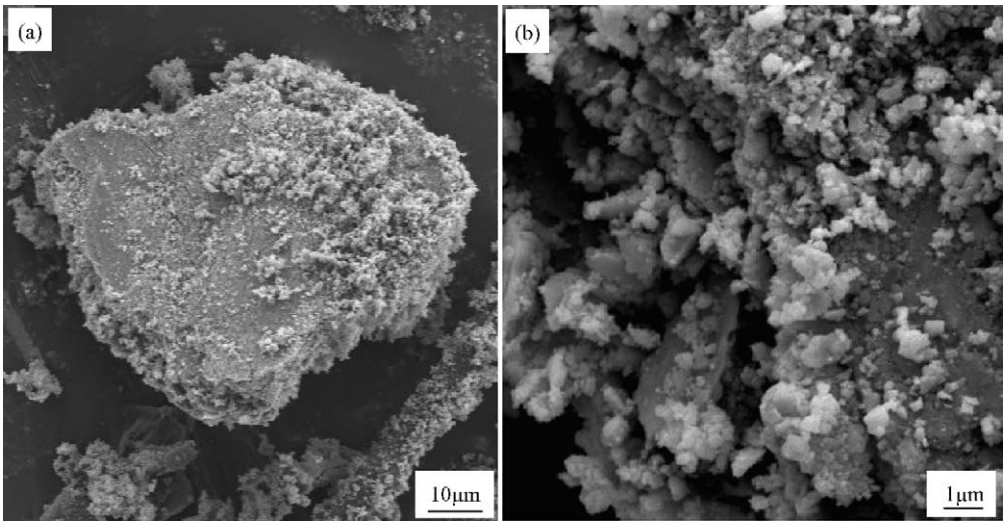

Fig. 10. SEM photographs of the wear debris for the C-30W_2B_5 composite tested at 75 N (a) plate-like debris and powdery debris (b) high magnified images of the cross section of the plate-like debris.

at low load. With increasing the applied load, the graphite-rich MML became more extensive and easier fracture and removal. As shown in Fig. 9(a) and (b), the area covered by the graphite-rich MML reduced (the uncovered area was the substrate surface left by the removal of the MML), the cracks on the MML became obvious and large pieces of flakes were being detached from the substrate. Even at 75 N (Fig. 9(c)), most of the worn surfaces were uncovered with the MML. The variation of the worn surfaces as the load increasing for the C-40W_2B_5 composite was similar to the C-30W_2B_5 composite.

Two types of morphologies were observed in the debris collected at 75 N for C-30W_2B_5 composite: powdery debris and plate-like debris, as exhibited in Fig. 10. The SEM photograph of the cross section of the plate-like debris showed that it was mainly comprised of ultrafine particles (Fig. 10(b)). Moreover, microcracks were present on the surface of the plate-like debris. EDX analysis noted that the plate-like debris was abundant in element of C (Fig. 11), which was in agreement with the composition of the MML on the worn surface of C-30W_2B_5. Such results strongly suggested that the plate-like debris was in fact detached from the MML

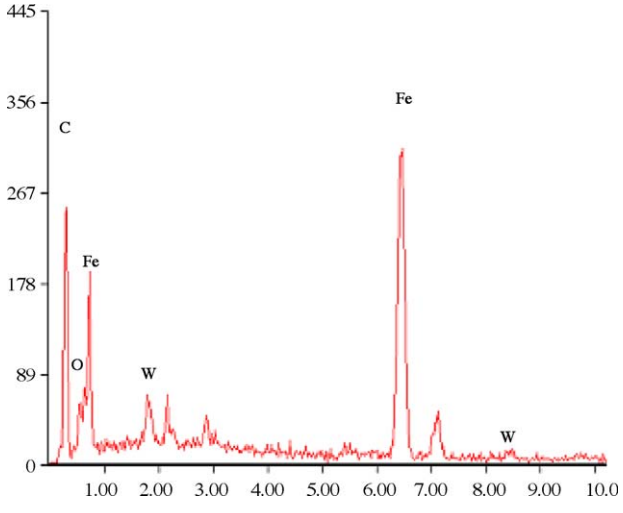

Fig. 11. EDX spectrum of the plate-like debris in Fig. 10(a).

4. Discussions

The present work has certificated that a MML containing elements from both sliding materials and environment was established during the sliding process of C-W_2B_5 composites against bearing steel. Because the MML contacted the counterface directly, the composition of the MML controlled the friction coefficient of the tribo-system, as discussed above. Moreover, a precondition for the wear of the composites was the removal of the MML. Therefore, it is important for the establishment, composition and failure of the MML to understand the friction and wear mechanisms.[21,22] In case of the relative simple configuration of carbon against metal, the carbon grain was broken down and smeared into a lubricant layer at the initial time. After a critical sliding, surface fatigue wear occurred.[16,17] In the case of ceramic against metal, fracture of surface ceramic grains and abrasive wear of the counterpart took place.[23] As it may be expected, the formation process of the MML for the carbon/ceramics composites worn against bearing steel should include breaking down and smearing of carbon grain, and cracking of ceramic grains and abrasive wear of the counterpart. The failure of the MML may also result from surface fatigue as carbon-graphite materials.

On the basis of above analysis and careful examination of the worn surface and wear debris, the establishment and failure of the MLL on the worn surface of the C-W_2B_5 composites are suggested as follows. In the initial stage of sliding wear, carbon grains were preferentially peeled by the asperities of the counterface and released on the worn surface as debris due to its softness and low strength. At the same time, a spot of iron debris was transferred from the counterface by micro cutting of the hard W_2B_5 grains, and microcracks in the W_2B_5 grains

were produced and gradually propagated. As sliding wear continued, W_2B_5 grains were cracked out on the worn surface as debris. The debris of carbon, Fe and W_2B_5 were subjected to a complicated process of fragmentation, mixing and compacting under normal load and frictional force to form aggregation. Most of the aggregation would progressively accumulate, mix up and smear on the sliding surface to create the MML, except for a small quantity of the aggregation detached from the worn surface. With further sliding, extensive mechanical mixing of materials from both contact surfaces would be involved in more areas on the surface.

Regarding the temperature rise as a result of frictional heat, the average temperature on the worn surface was found to increase with the W_2B_5 content. At 75 N, the average surface temperatures were about 298 K, 365 K and 395 K for the graphite, C-30W_2B_5 and C-40W_2B_5 composites, respectively. Although the bulk surface temperature was not very high because of the lower friction coefficient, the local flash temperature at real contact asperities of hard W_2B_5 and Fe could be much higher, which caused the oxidation of the very fine W_2B_5 and iron debris since the wear system was exposed to air.

After critical cycles of compressive stress and tangential stress arising from the combined action of normal load and frictional force, the surface fatigue occurred which was associated with fracture of the grains in the subsurface leading to a weakening of the adhesion of the layer to its substrate.[16,17] As a result, microcracks propagated in the MML and the MML-substrate interface[16] resulting in breaking away of partial MML as flaky debris. Some of the flaky debris were scaled off the worn surface, and the others would undergo further rubbing on the worn surface. The fresh materials exposed on the wear surface may participate in the following friction process and form a new MML. It is this process of formation and failure of the MML that controls the wear process of the composite.

The notable increase of fracture toughness of the C-W_2B_5 composites, as shown in Table 1, dramatically improved their wear resistance compared to neat graphite because, under certain shearing stress, high fracture toughness can hinder both the fracture of grains in the subsurface and the cracks propagation, therefore retarding surface fatigue. However, the wear rate of the C-40W_2B_5 composite was a little higher than that of the C-30W_2B_5 composite, which was ascribed to the higher frictional force of C-40W_2B_5 composite producing higher shearing stress. Analysis of the Hertzian stress fields produced during the wear test, using the method described by Smith and Liu,[24] indicated the maximum shearing stress for the C-40W_2B_5 composite (~310 MPa) was about 30% higher than that for the C-30W_2B_5 composite (~240 MPa) at normal load of 75 N.

5. Conclusions

Based on the investigation of the mechanical properties and friction and wear behavior of the C-W_2B_5 composites and graphite, the following conclusions can be obtained.

The C-W_2B_5 composites are synthesized via an in situ reaction sintering route from B_4C, WC and carbon black powders, by hot-pressing at 2000 °C and 25 MPa for 1 h. The addition of W_2B_5 significantly improved the mechanical properties of the composites compared with neat graphite. The flexural strength and fracture toughness of the C-40W_2B_5 composite were about four and seven times that of graphite, respectively. The high relative density, hard W_2B_5 grains and residual stress are believed to contribute to the strengthening and toughening of the composites.

The compositions of the materials and the testing loads have great effects on the friction coefficient and wear rate of the C-W_2B_5 composites. The friction coefficients increased with increasing W_2B_5 content and normal loads, while the friction coefficient of the C-30W_2B_5 composite was very close to graphite. The composites had much lowered wear rates as compared with graphite. A mechanically mixed layer containing elements from the friction counterparts and environment was formed on the worn surface. The composition of the MML and fracture toughness of the composites played a very important role in both friction coefficient and wear rate. The very low friction coefficient and wear rate of the C-30W_2B_5 composite was attributed to the presence of graphite-rich MML and increased toughness. The higher friction coefficient of the C-40W_2B_5 composite resulting from the increase of hard W_2B_5 grains increased the maximum shearing stress, hence increasing wear rate in spite of the higher fracture toughness. The fracture and removal of the MML are considered to be the main wear mechanism of the C-W_2B_5 composites.

Acknowledgments

The authors gratefully thank associate Prof. Q.C. Meng, J.C. Rao for helping us in TEM studies, and Mr. B.Y. Zhang for taking SEM photographs and Mr. H.Z. Xia and Mrs. X.R. Liu for taking XRD patterns.

References

[1]. Fitzer, E., Future of carbon-carbon composites. *Carbon*, 1987, **25**(2), 163–190.
[2]. Liu, S. J. and Sun, J., Corrosion resistant graphite and graphite sealing. *Polyester Ind.*, 2001, **14**, 61–62 [in Chinese].
[3]. Leefe, S., Seals research to boost rocket engines into the 21st century sealing technology. *Sealing Technol.*, 1998, **53**, 7–9.
[4]. Song, Y. Z., Zhai, G. T., Li, G. S., Shi, J. L., Guo, Q. G. and Liu, L., Carbon/graphite seal materials prepared from mesocarbon microbeads. *Carbon*, 2004, **42**, 1427–1433.
[5]. Miyazaki, K., Hagio, T. and Kobayashi, K., Graphite and boron carbide composites made by hot-pressing. *J. Mater. Sci.*, 1981, **16**, 752–762.
[6]. Ogawa, I., Preparation of carbon/ceramic composite materials by use of raw coke. Part 9. Mechanical and thermal properties of C/SiC/B_4C composites. *J. Ceram. Soc. Jpn.*, 1994, **102**(10), 976–981.
[7]. Guo, Q. G., Song, J. R., Liu, L. and Zhang, B. J., Factors influencing oxidation resistance of B_4C/C composites with self-healing properties. *Carbon*, 1998, **36**(11), 1597–1601.
[8]. Wen, G., Li, S. B., Zhang, B. S. and Guo, Z. X., Processing of in situ toughened B-W-C composites by reaction hot pressing of B_4C and WC. *Script. Mater.*, 2000, **43**, 853–857.
[9]. Liang, Y. J. and Che, M. C., *Hand Book of the Thermodynamic data for Inorganic Material*, *65*. North East University Press, PR China, 1993, p. 419.

[10]. Duschanek, H. and Rogl, P., Critical assessment and thermodynamic calculation of the binary system Boron-Tungsten (B-W). *J. Phase Equilibr.*, 1995, **16**(2), 150–161.

[11]. Deng, J. X., Zhou, J., Feng, Y. H. and Ding, Z. L., Microstructure and mechanical properties of hot-pressed B_4C/(W Ti) C ceramic composites. *Ceram. Int.*, 2002, **28**, 425–430.

[12]. Ohya, Y., Hoffmann, M. J. and Petzow, P., Sintering of in-situ synthesized SiC-TiB_2 composites with improved fracture toughness. *J. Am. Ceram. Soc.*, 1992, **75**(9), 2479–2483.

[13]. Taya, M., Hayashi, S., Kobayashi, A. S. and Yoon, H. S., Toughening of a particulate-reinforced ceramic-matrix composite by thermal residual stress. *J. Am. Ceram. Soc.*, 1990, **73**(5), 1382–1391.

[14]. Zhang, G. J., Guo, Q. G., Liu, Z. J., Yao, L. Z. and Liu, L., Effects of dopants on properties and microstructure of doped graphite. *J. Nucl. Mater.*, 2002, **301**, 187–192.

[15]. Nagaoka, T., Yasuoka, M. and Hirao, K., Effect of TiN particle size on mechanical properties of Si_3N_4/TiN particulate composites. *J. Ceram. Soc. Jpn.*, 1992, **100**(1160), 617–620.

[16]. Clark, W. T. and Lancaster, J. K., Breakdown and surface fatigue of carbons during repeated sliding. *Wear*, 1963, **6**, 467–482.

[17]. Blaw, P. J. and Martin, R. L., Friction and wear of carbon-graphite materials against metal and ceramic counterfaces. *Tribol. Int.*, 1994, **27**, 413–422.

[18]. Zhan, Y. Z. and Zhang, G. D., Friction and wear behavior of copper matrix composites reinforced with SiC and graphite particles. *Tribol. Lett.*, 2004, **17**, 91–98.

[19]. Ted-Guo, M. L. and Tsao, C. Y. A., Tribological behavior of self-lubricating aluminium/SiC/graphite hybrid composites synthesized by the semi-solid powder-densification method. *Compos. Sci. Technol.*, 2000, **60**, 65–74.

[20]. Blau, P. J., Dumont, B., Braski, D. N., Jenkins, T., Zanoria, E. S. and Long, M. C., Reciprocating friction and wear behavior of a ceramic-matrix graphite composite for possible use in diesel engine valve guides. *Wear*, 1999, **225–229**, 1338–1349.

[21]. Rigney, D. A., Chen, L. H. and Naylor, M. G. S., Wear processes in sliding systems. *Wear*, 1984, **100**, 195–219.

[22]. Li, X. Y. and Tandon, K. N., Mechanical mixing induced by sliding wear of an Al–Si alloy against M2 steel. *Wear*, 1999, **225–229**, 640–648.

[23]. Kameo, K., Friedrich, K., Bartolomé, J. F., Díaz, M., López-Esteban, S. and Moya, J. S., Sliding wear of ceramics and cermets against steel. *J. Eur. Ceram. Soc.*, 2003, **23**, 2867–2877.

[24]. Smith, J. O. and Liu, C. K., Stresses due to tangential and normal loads on an elastic solid with application to some contact stress problems. *ASMF Trans.*, 1953, **75**, 157–165.